DOI: 10.1002/chem.200500849

Chalcogenide Derivatives of Imidotin Cage Complexes

Dana J. Eisler and Tristram Chivers*[a]

Abstract: Reaction of the secocubane $[Sn_3(\mu_2\text{-}NHtBu)_2(\mu_2\text{-}NtBu)(\mu_3\text{-}NtBu)]$ (**1**) with dibutylmagnesium produces the heterobimetallic cubane $[Sn_3Mg(\mu_3\text{-}NtBu)_4]$ (**4**) which forms the monochalcogenide complexes of general formula $[ESn_3Mg(\mu_3\text{-}NtBu)_4]$ (**5a**, E = Se; **5b**, E = Te) upon reaction with elemental chalcogens in THF. By contrast, the reaction of the anionic lithiated cubane $[Sn_3Li(\mu_3\text{-}NtBu)_4]^-$ with the appropriate quantity of selenium or tellurium leads to the sequential chalcogenation of each of the three Sn^{II} centres. Pure samples of the mono- or dichalcogenides are, however, best obtained by stoichiometric redistribution reactions of $[Sn_3Li(\mu_3\text{-}NtBu)_4]^-$ and the trichalcogenides $[E_3Sn_3Li(\mu_3\text{-}NtBu)_4]^-$ (E = Se, Te). These reactions are conveniently monitored by using ^{119}Sn NMR spectroscopy. The anion $[Sn_3Li(\mu_3\text{-}NtBu)_4]^-$ also acts as an effective chalcogen-transfer reagent in reactions of selenium with the neutral cubane $[\{Sn(\mu_3\text{-}N(dipp)\}_4]$ (**8**) (dipp = 2,6-diisopropylphenyl) to give the dimer $[(thf)Sn\{\mu\text{-}N(dipp)\}_2Sn(\mu\text{-}Se)_2Sn\{\mu\text{-}N(dipp)\}_2Sn(thf)]$ (**9**), a transformation that results in cleavage of the Sn_4N_4 cubane into four-membered Sn_2N_2 rings. The X-ray structures of **4**, **5a**, **5b**, $[Sn_3Li(thf)(\mu_3\text{-}NtBu)_4(\mu_3\text{-}Se)(\mu_2\text{-}Li)(thf)]_2$ (**6a**), $[TeSn_3Li(\mu_3\text{-}NtBu)_4][Li(thf)_4]$ (**6b**), $[Te_2Sn_3Li(\mu_3\text{-}NtBu)_4][Li([12]crown\text{-}4)_2]$ (**7b″**) and **9** are presented. The fluxional behaviour of cubic imidotin chalcogenides and the correlation between NMR coupling constants and tin–chalcogen bond lengths are also discussed.

Keywords: chalcogens · cluster compounds · cubanes · multiple bonds · tin

Introduction

The chemistry of complexes involving terminal linkages between heavy Group 14 and Group 16 elements has undergone impressive developments since the discovery of the first examples more than ten years ago.[1] The reactive M=E (M = Ge, Sn or Pb; E = Se or Te) functionality exhibits a propensity to dimerise as a result of its polar character (resonance form **A**). Two strategies have been employed successfully to inhibit this tendency.

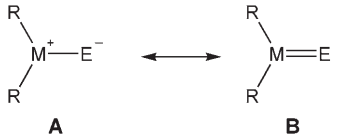

The first approach involves the kinetic stabilisation of the multiple (terminal) bond through the use of extremely bulky substituents attached to M. This strategy generates derivatives with three-coordinate metal centres that are genuine analogues of ketones.[2,3] The second method uses intramolecular coordination of heteroatoms, such as nitrogen, to the Group 14 centre in order to reduce the polarity of the terminal bond. This approach, which produces complexes in which the metal centre is four or five coordinate, has provided the first examples of stannanetellurones.[4,5] It has also been used to prepare the first examples of complexes containing two or three M=Se bonds, namely $[Sn_4Se_2(\mu_3\text{-}NtBu)_4]$ and $[Ge_4Se_3(\mu_3\text{-}NtBu)_4]$, respectively,[6] by the direct reaction of the cubanes $[M_4(\mu_3\text{-}NtBu)_4]$ with chalcogens. Our interest in these systems stems from the notion that imidotin complexes of the type $[Sn_4E_4(\mu_3\text{-}NtBu)_4]$, in which all the metal centres are chalcogenated, might serve as single-source precursors for the low-band-gap semiconductors SnE (E = Se, Te) through the thermodynamically favoured elimination of the diazene tBuN=NtBu.[7,8] In view of the limited reactivity of the neutral cubane $[Sn_4(\mu_3\text{-}NtBu)_4]$ towards chalcogens,[6] we decided to adopt a different strategy based on our earlier finding that previously inaccessible P–Te ligands can be prepared from precursors that incorporate an N–H functionality by the generation of anionic species (through metallation

[a] Dr. D. J. Eisler, Prof. T. Chivers
Department of Chemistry
University of Calgary
Calgary, AB T2N 1N4 (Canada)
Fax: (+1) 403-289-9488
E-mail: chivers@ucalgary.ca

with NaH or *n*BuLi) prior to reaction with tellurium.[9] Application of this methodology to imidotin systems involves the use of the amido/imido secocube **1** reported by Veith

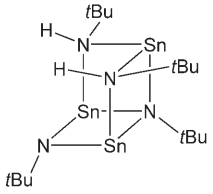

1

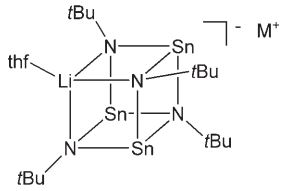

2a: M = $Li(thf)_4$
2a': M = (thf)Li([12]crown-4)

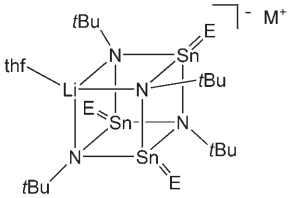

3a: M = $Li(thf)_4$, E = Se
3a': M = (thf)Li([12]crown-4), E = Se
3b: M = $Li(thf)_4$, E = Te

et al.[10] In a preliminary communication we disclosed the synthesis of the dilithiated complexes **2a** and **2a′** and showed that their reactions with chalcogens occur rapidly under mild conditions to give the corresponding trichalcogenides **3a**, **3a′** and **3b**, whose X-ray structures were reported.[11] In this full account we describe 1) the magnesiation of **1** and a comparison of the reactivity of the magnesium derivative towards chalcogens with that of **2**, 2) the characterisation of the mono- and dichalcogeno derivatives of **2** by means of X-ray crystallography and multinuclear NMR spectroscopy, 3) the use of **2a** as a chalcogen-transfer agent for the selenation of recalcitrant imidotin cubanes, for example, [{Snμ_3-N(dipp)}$_4$], which, unexpectedly, results in cleavage of the Sn_4N_4 cage to give Sn_2N_2 rings and 4) the employment of ^{119}Sn NMR spectroscopy to monitor these chalcogenation reactions. The fluxional behaviour of imidotin chalcogenides is also discussed in the context of multinuclear NMR studies. Finally, the relationship between tin–chalcogen NMR coupling constants and bond lengths is analysed by means of a comparison of the current results with data available in the literature.

Results and Discussion

Reactions of magnesium and lithium derivatives of 1 with chalcogens: Magnesiation of **1** with dibutylmagnesium in hot THF results in the formation of the neutral heterobimetallic cubane complex **4** in good yield as outlined in Scheme 1. The monochalcogenide complexes **5a** and **5b** are

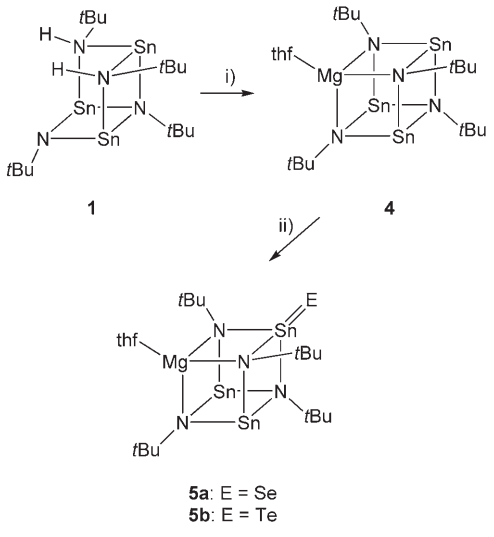

Scheme 1. Synthesis of [$Sn_3Mg(\mu_3$-N*t*Bu)$_4$] (**4**) and monochalcogenide complexes **5a** and **5b**. i) Bu_2Mg, THF, 60 °C, 16 h. ii) Se, THF, 25 °C, 1 h; Te, THF, 40 °C, 3 h.

readily prepared by reaction of **4** with one equivalent of the appropriate elemental chalcogen at mild temperatures (Scheme 1). The reaction of **4** with more than one equivalent of selenium results in the formation of gel-like solutions from which only insoluble products can be obtained. A similar observation was made for the reaction of **1** with selenium,[12] and is presumably an indication of the formation of oligomeric or polymeric complexes with bridging selenido ligands. Complex **4** does not react further with excess tellurium; even in boiling THF only the monotelluride **5b** is obtained. The lower reactivity of magnesium derivative **4** towards chalcogens, relative to that of lithium derivatives **2** (see below), parallels our earlier observations for the reactions of the [*t*BuNP(μ-N*t*Bu)$_2$PN*t*Bu]$^{2-}$ anion towards tellurium.[13]

The reaction of the anionic lithium-containing cubane **2a** with one equivalent of elemental chalcogen rapidly produces the monochalcogenide complexes **6a** and **6b** as depicted in Scheme 2. However, owing to the highly reactive nature of **2a**, it is difficult to prepare pure samples of the monochalcogenides using this method. The NMR spectra of the isolated products showed the presence of small quantities of dichalcogenide complexes **7a** or **7b**, indicating that even a very small excess of chalcogen results in the immediate formation of complexes **7** (Figure 1). Similar difficulties are encountered when employing this methodology to prepare the dichalcogenide complexes **7a** and **7b**, owing to contamination by the trichalcogenated complexes **3a** and **3b**, respectively.

Chalcogen-transfer reactions: As reported previously, the fully chalcogenated complexes **3** readily transfer chalcogens to Sn^{II} centres of the parent clusters **2**.[11] This chalcogen-exchange process allows for a more convenient synthesis of pure samples of partially chalcogenated complexes through stoichiometric reactions of complexes **3** and **2**, exemplified

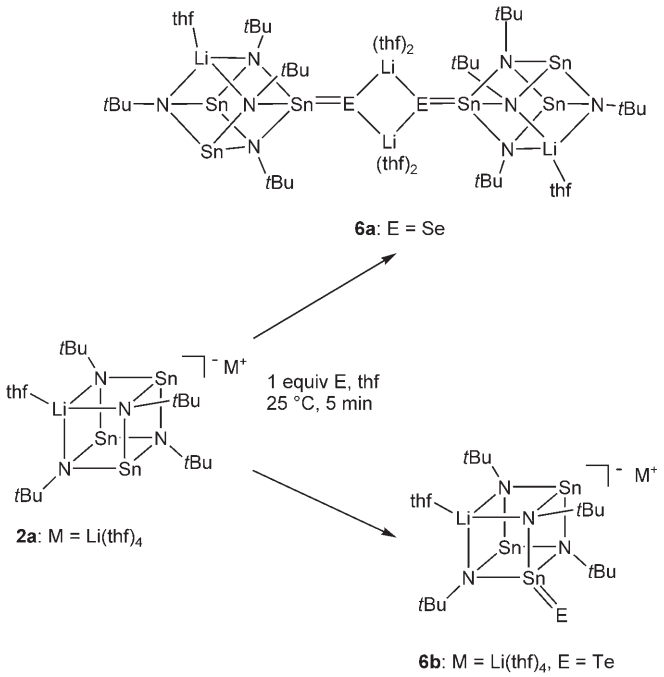

Scheme 2. Synthesis of monochalcogenide complexes **6a** and **6b**.

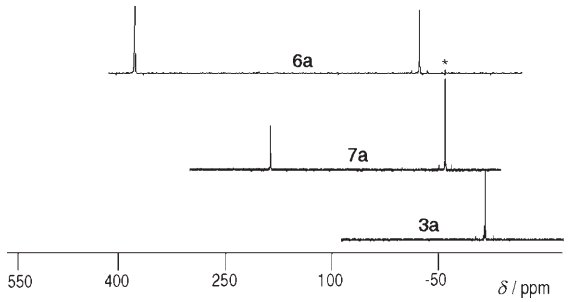

Figure 1. ^{119}Sn NMR spectra of **6a**, **7a** and **3a**. The asterisk (*) indicates the presence of trace amounts of the diselenide **7a** in the sample of the monoselenide **6a**.

by the formation of complexes **7a** and **7b** as outlined in Scheme 3 (also shown in Figure 1).

The ease of this chalcogen exchange suggests the possibility of adapting this process to generate imidotin clusters with different terminal chalcogen atoms. Indeed, the reaction of the triselenide **3a** with the tritelluride **3b** results in the immediate formation of mixed chalcogenide derivatives; however, a complex mixture of products is obtained as evidenced by multinuclear NMR spectra. Monitoring of the reaction solution over several days demonstrated that the mixed Se/Te complexes remain in equilibrium, and no single product is preferred. Similar difficulties were obtained when attempting to prepare mixed complexes by the reaction of partially chalcogenated complexes **6** and **7** with elemental chalcogens, for example, in the reaction of the diselenide complex **7a** with one equivalent of tellurium to prepare $[Se_2TeSn_3Li(NtBu)_4]^-$. Although it was possible to obtain single crystals from the reaction mixtures, X-ray diffraction

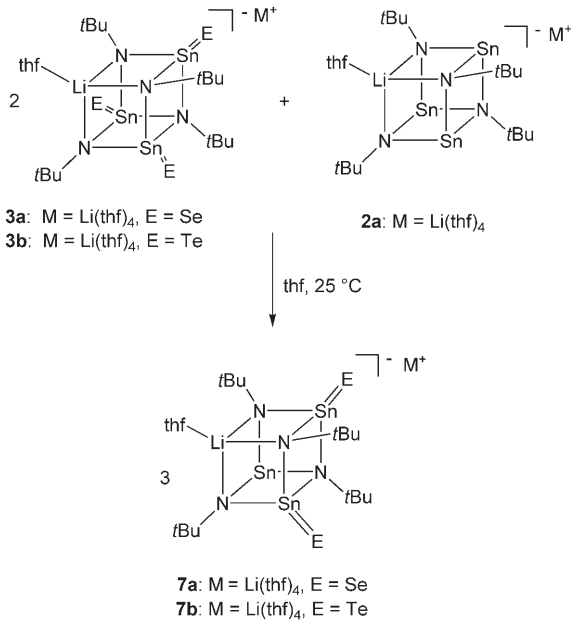

Scheme 3. Synthesis of dichalcogenide complexes **7a** and **7b** by the redistribution reaction of complexes **3** and **2**.

analyses revealed that the crystals were a mixture of selenium- and tellurium-containing cage complexes that had co-crystallised.

The facile chalcogen exchange observed for complexes **3** prompted us to investigate their use as chalcogen-transfer reagents with substrates that are difficult to chalcogenate. The neutral cubane $[\{SnN(dipp)\}_4]$ (**8**) (dipp = 2,6-diisopropylphenyl) does not react with elemental selenium either at room temperature in THF or in boiling toluene. However, the addition of a catalytic amount of **3a** (generated in situ) to a mixture of **8** and selenium results in quantitative formation of the dimeric complex **9** (see below) at room temperature after 24 hours as shown in Scheme 4. The phosphane

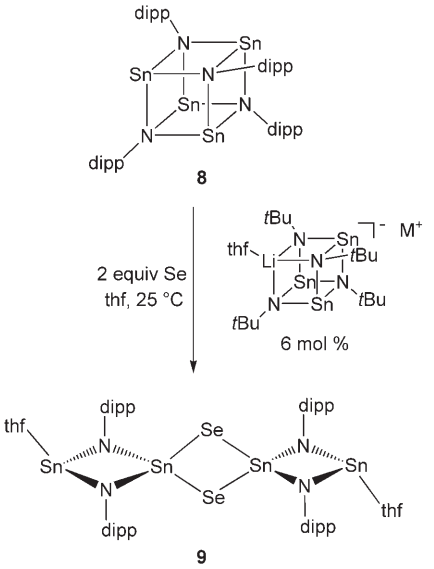

Scheme 4. Synthesis of dimeric complex **9**.

$P(NMe_2)_3$ performs a catalytic role in certain reactions of elemental selenium, for example, insertion into Al–H bonds.[14] The transformation of the Sn_4N_4 cube into four-membered Sn_2N_2 rings during this process is, to our knowledge, unprecedented in reactions of imidotin tetramers. The X-ray structure of [{SnN(dipp)}$_4$] has been reported and the germanium analogue forms a six-membered ring in preference to a cubane.[15] However, Veith and Frank have shown that dimeric $(SnNR)_2$ units may be trapped by addition of $Sn(OtBu)_2$, for example, in the formation of [{Sn(μ-N*t*Bu)}$_2$Sn(O*t*Bu)$_2$].[16] The formation of **9** formally involves the uptake of two Se atoms for each molecule of **8**. Two pathways (denoted **I** and **II** in Scheme 5) could account for

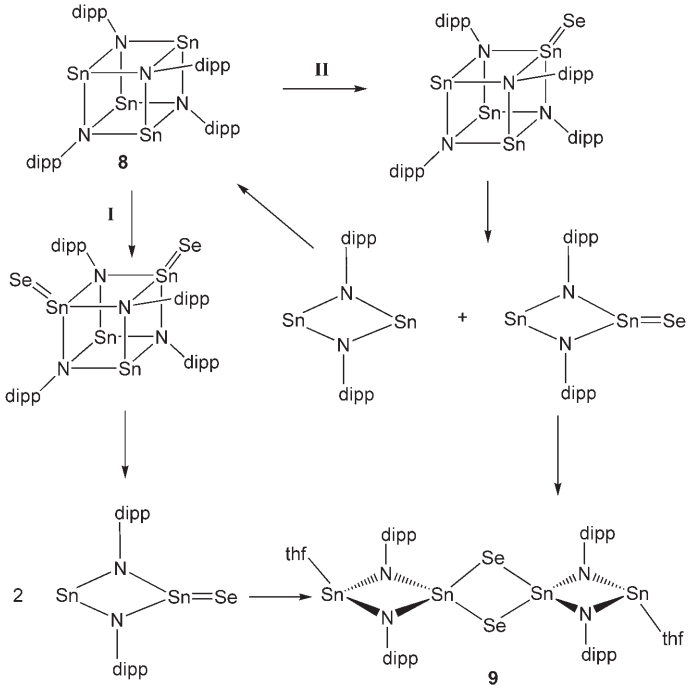

Scheme 5. Possible pathways leading to the formation of complex **9**.

the production of dimer **9**. Pathway **I** invokes the initial formation of the diselenide [Sn_4Se_2{N(dipp)}$_4$] followed by dissociation of the Sn_4N_4 cube into two Sn_2N_2 rings. For comparison, we note that the *tert*-butyl derivative [Sn_4Se_2-(N*t*Bu)$_4$] does not dissociate.[6] Alternatively, **9** may be formed by dissociation of the initially formed monoselenide [Sn_4Se{N(dipp)}$_4$] as depicted in pathway **II** (Scheme 5). Subtle changes in the electronic properties of the tin cage can have a marked influence on the stability of complexes containing a terminal Sn=E bond (E = S, Se, Te).[17] We have previously reported that the monoselenide [$Sn_3Se(\mu_2$-NH*t*Bu)$_2$(μ_2-N*t*Bu)(μ_3-N*t*Bu)] engages in a monomer–dimer equilibrium in solution.[12] The dimerisation of the monoselenide [Sn_4Se{N(dipp)}$_4$] would generate five-coordinate tin centres with three bulky N(dipp) neighbours. Subsequently, the dissociation of the Sn_4N_4 cube into two Sn_2N_2 rings may occur to alleviate this steric strain. Both pathways **I** and **II** lead to the monomeric selenone [Sn{μ-N(dipp)}$_2$Sn=Se], with a three-coordinate tin centre, which would dimerise spontaneously to give **9**. Attempts to prepare tellurium derivatives of **8** by reaction with tellurium using a catalytic amount of **2a** were unsuccessful, even at elevated temperatures. Presumably the lack of reaction is a result of the low susceptibility towards oxidation of the tin centres in **8** combined with the lower oxidising power of tellurium relative to selenium.

X-ray structures: The X-ray structure of complex **4** is depicted in Figure 2 with selected bond lengths and angles given

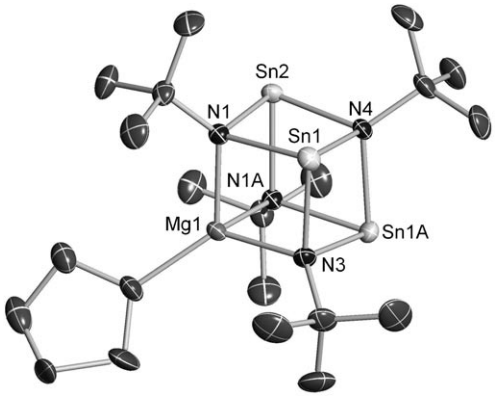

Figure 2. Molecular structure of complex **4**. Thermal ellipsoids are shown at 30% probability. Hydrogen atoms have been removed for clarity.

in Table 1. The Sn_3MgN_4 core is a distorted cubane, with the magnesium centre occupying the previously empty corner of secocubane **1**. The Mg^{II} centre is bound to three nitrogen atoms, with a molecule of THF completing the coordination sphere. The bond angles around Mg deviate considerably from ideal tetrahedral values, ranging from 91.4(1) to 125.3(2)°. The range of Sn^{II}–N distances (2.188(2)–2.205(3) Å) is typical of those observed in other Sn^{II} cubane structures.[10,15] The bond angles around the Sn^{II} centres (81.7(1)–84.7(1)°) reflect the stereochemical influence of the lone pairs on the Sn^{II} centres.

The structures of the monochalcogenides **5a** and **5b** were determined by means of X-ray crystallography and in each case were found to contain a terminal Sn=E bond (Figure 3). The Sn=Se distance of 2.393(1) Å (Table 1) in **5a** falls in the range for reported Sn=Se bond lengths (2.363(1)–2.418(1) Å).[5,6,18] For complex **5b**, the Sn=Te distance of 2.611(1) Å (Table 1) is comparable to the Sn=Te distance of 2.618(1) Å observed in the five-coordinate complex [SnTe{CH(SiMe$_3$)C$_9$H$_6$N-8}$_2$].[18c] There is a lengthening of the Sn=E bonds found in **5a** and **5b** in comparison with those in the related neutral complexes [$Sn_4Se_2(\mu_3$-N*t*Bu)$_4$] and [$Sn_4Te(\mu_3$-N*t*Bu)$_4$] (2.367(1) Å, E = Se; 2.589(1) Å, E = Te), however, the N–Sn^{IV} distances are identical within experimental error.[6] Presumably, the lengthening of the Sn=E bonds is due to a subtle change in the electronic properties of the cage complex as a result of the replacement of one tin centre with the more electropositive magnesium centre.

Table 1. Selected bond lengths [Å] and angles [°] for complexes **4**, **5a**, **5b**, **6a**, **6b** and **7b″**.

	4	**5a**	**5b**	**6a**	**6b**	**7b″**
Sn1–E1[a]		2.393(1)	2.611(1)	2.452(1)	2.640(1)	2.614(1)[d]
Sn1–N1	2.191(2)	2.122(4)	2.117(3)	2.055(3)	2.068(5)	2.057(8)
Sn1–N3	2.188(2)	2.114(4)	2.110(3)	2.056(3)	2.072(5)	2.06(1)
Sn1–N4	2.201(2)	2.134(4)	2.119(3)	2.115(3)	2.138(5)	2.150(8)
Sn2–N1	2.192(2)	2.222(4)	2.233(3)	2.174(3)	2.169(5)	2.122(8)
Sn2–N2[b]		2.183(5)	2.190(3)	2.136(3)	2.136(5)	2.10(1)
Sn2–N4	2.205(3)	2.223(5)	2.232(3)	2.237(3)	2.235(5)	2.192(9)
Sn3–N2		2.177(5)	2.187(3)	2.140(4)	2.142(5)	2.17(1)
Sn3–N3		2.231(4)	2.230(3)	2.191(3)	2.181(5)	2.19(1)
Sn3–N4		2.229(5)	2.239(3)	2.248(3)	2.227(5)	2.282(9)
M1[c]–N1	2.060(2)	2.100(5)	2.092(4)	2.160(8)	2.16(1)	2.14(2)
M1[c]–N2		2.046(5)	2.063(3)	2.071(8)	2.10(1)	2.13(2)
M1[c]–N3	2.061(4)	2.095(5)	2.095(3)	2.162(8)	2.13(1)	2.13(2)
N1-Sn1-E1[a]		128.0(1)	128.6(1)	125.3(1)	127.1(1)	124.5(2)[c]
N1-Sn1-N3	84.7(1)	88.4(2)	87.5(1)	95.7(1)	93.8(2)	91.4(4)
N1-Sn1-N4	81.8(1)	85.3(2)	86.1(1)	86.1(1)	85.6(2)	86.2(3)
N3-Sn1-N4	82.0(1)	85.8(2)	85.6(1)	86.8(1)	85.4(2)	86.0(4)
N1-Sn2-N2	84.5(1)[b]	83.5(2)	84.1(1)	87.9(1)	89.0(2)	92.5(4)
N1-Sn2-N4	81.7(1)	80.9(2)	80.7(1)	80.4(1)	80.9(2)	83.5(3)
N2-Sn2-N4		81.7(2)	81.7(1)	81.5(1)	81.3(2)	85.5(4)
N2-Sn3-N3		84.0(2)	83.9(1)	88.6(1)	88.1(2)	90.9(4)
N2-Sn3-N4		81.7(2)	81.7(1)	81.2(1)	81.3(2)	81.9(3)
N3-Sn3-N4		80.8(2)	80.1(1)	80.4(1)	80.8(2)	79.8(3)

[a] For complexes **5a** and **6a** E = Se, and for **5b**, **6b** and **7b″** E = Te. [b] For complex **4**, N2 is the symmetry equivalent of N1 (N1A). [c] For complexes **4**, **5a** and **5b** M = Mg, and for **6a**, **6b**, **7b″** M = Li. [d] Sn2–Te2 2.615(1) Å; N1-Sn2-Te2 123.9(2)°.

The Sn^{IV}–N distances in both complexes **5a** and **5b** are considerably shorter than the Sn^{II}–N distances, as observed in other imidotin cubane chalcogenide complexes;[6,11] this behaviour reflects the higher ionic character of the Sn^{IV}–N bonds. The N-Sn^{IV}-N bond angles are larger (85.3(2)–88.4(2)°) than the N-Sn^{II}-N angles (80.1(1)–84.1(1)°) as a result of the stereochemical influence of the lone pairs on the Sn^{II} centres.

The crystal structure determination of the monoselenide **6a** revealed that, in the solid state, the complex is present as the dimeric species depicted in Figure 4. The dimer consists of two monoanionic imidotin cage complexes, each of which contains a terminal tin–selenium bond, that are associated by two bridging $Li(thf)_2^+$ units. Thus, the solid-state structure of **6a** can be considered as arising from the dimerisation of two contact ion pairs. The Sn=Se bond length of 2.452(1) Å is considerably longer than the longest Sn=Se bond reported (2.418(1) Å),[5] but shorter than typical Sn–Se single bonds (2.55–2.60 Å),[19] behaviour suggesting a significant amount of multiple bond character. The long Sn=Se distance present in the structure of **6a** can be interpreted as the result of a substantial contribution from resonance structure **A** (see above), which is further evinced by the Sn^{IV}–N distances. The two imido groups, which are bound to the Sn^{IV} centre as well as to the cage lithium cation, exhibit significantly shorter Sn^{IV}–N bond lengths (2.055(3), 2.056(3) Å) in comparison with complex **5a** (Table 1). The bond contractions suggest that a substantially higher positive charge resides on the Sn^{IV} centre in **6a**. Furthermore, the association of the noncage lithium cation with the cluster, forming a contact ion pair, suggests a significant amount of negative charge is present on the selenium atoms. Both of these observations are in keeping with the bonding description depicted by resonance structure **A**. By comparison, the analogous Sn^{IV}–N distances in the fully chalcogenated cluster **3a′** are longer, ranging from 2.082(4)–2.105(4) Å, while the Sn=Se distances are shorter (mean 2.39(1) Å).[11] Thus it appears that there is significant localisation of the anionic charge of the imidotin cluster in **6a** which greatly increases the contribution of **A** to the Sn=Se bonding. Presumably the long Sn=Se bond is in part due to the Li–Se bonding interactions, however, the anionic nature of the imidotin cluster is likely the most significant contributor to the observed bond lengthening. The molecular structure obtained for monotelluride **6b** (Figure 5) provides considerable support for this rationale.

In contrast to **6a**, monotelluride **6b** is monomeric in the solid state and is present as a solvent-separated ion pair. The terminal Sn=Te bond length of 2.640(1) Å is longer than any reported terminal Sn=Te distance, the longest previously being 2.618(1) Å.[18c] Clearly, the considerable lengthening of the Sn=Te bond in **6b** must be due to the electronic nature of the monoanionic imidotin cage, as there are no significant interactions with the $Li(thf)_4^+$ cation (Te···Li = 4.87 Å). The two lithium-associated Sn^{IV}–N distances of 2.068(5) and 2.072(5) Å in **6b** are shorter than the analogous bonds in **5b** (Table 1), but longer than those observed in **6a**. Presumably these observations reflect a reduction of the contribution of resonance structure **A** to the Sn=E bonding as a result of the lower electronegativity of Te relative to Se.

The crystal structure of ditelluride **7b″** was determined by means of X-ray crystallography and the anion is shown in Figure 6. The two terminal Sn=Te bond lengths are indistinguishable within error ((2.614(1), 2.615(1) Å, Table 1), and are considerably shorter than that observed in **6b**. Furthermore, the Sn=Te distances in **7b″** are slightly longer than the average Sn=Te distance of 2.607(1) Å observed in the structure of **3b**.[11] It is worth noting that in the structure of **3b**, there are six molecules in the asymmetric unit, providing 18 Sn=Te distances that range from 2.600(1)–2.613(1) Å. Thus, the Sn=Te distances observed in **7b″** are comparable to the longest distances observed in **3b**. The lithium associated Sn^{IV}–N bond lengths in **7b″** range from 2.057(8) to

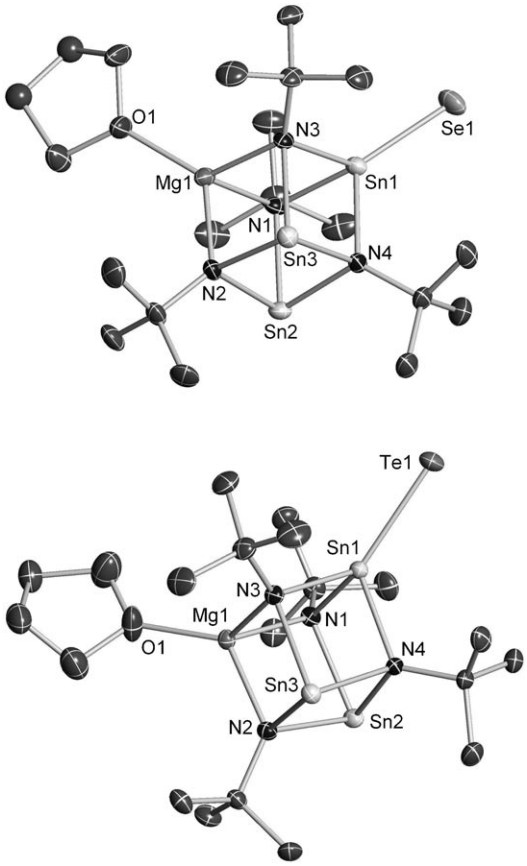

Figure 3. Molecular structures of **5a** (top) and **5b** (bottom). Thermal ellipsoids are shown at 30% probability. Hydrogen atoms have been removed for clarity.

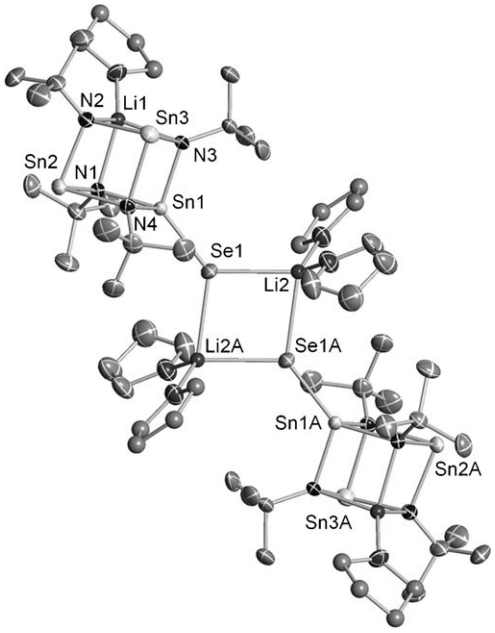

Figure 4. Molecular structure of complex **6a**. Thermal ellipsoids are shown at 30% probability. Hydrogen atoms have been removed for clarity.

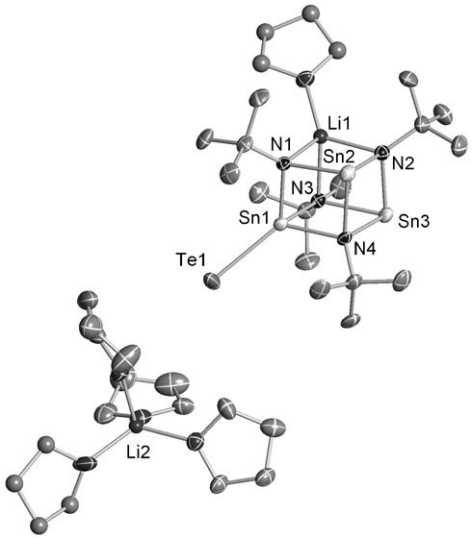

Figure 5. Molecular structure of complex **6b**. Thermal ellipsoids are shown at 30% probability. Hydrogen atoms have been removed for clarity.

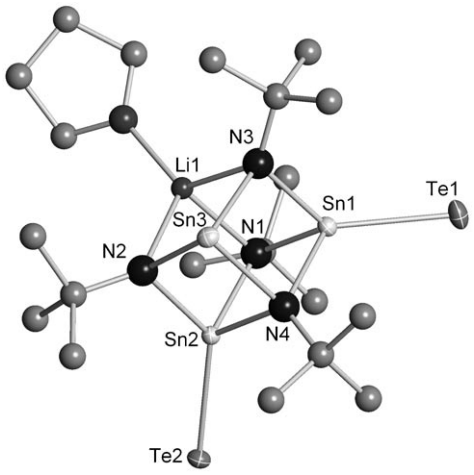

Figure 6. Molecular structure of the anion in complex **7b**″. Thermal ellipsoids are shown at 30% probability. Hydrogen atoms have been removed for clarity.

2.122(8) Å, and are similar to those observed for tritelluride **3b** (2.07(1)–2.12(1) Å). These data suggest that there is some delocalisation of the charge over the two Sn^{IV} centres in **7b**″, resulting in a further reduction in the contribution of resonance structure **A** (relative to **6b**). Presumably, in the case of **3b** there is delocalisation of the anionic charge over all three Sn^{IV} centres, thereby minimising the ionic character of the Sn=Te bonds; this results in the shortest Sn=Te distances observed for this series of stannatellurones.

There are two independent, but chemically equivalent molecules present in the crystal structure of complex **9** that have similar metrical parameters (Table 2) and so only one molecule is depicted in Figure 7. The structure of complex **9** can be viewed to be comprised of three interconnected four-

Table 2. Selected bond lengths [Å] and angles [°] for complex **9**.

Molecule 1		Molecule 2	
Sn1–Se1	2.555(3)	Sn3–Se2	2.519(3)
Sn1–Se1A	2.532(3)	Sn3–Se2A	2.557(3)
Sn1–N1	2.03 (2)	Sn3–N3	2.03 (2)
Sn1–N2	2.00(2)	Sn3–N4	2.04(2)
Sn2–N1	2.12(2)	Sn4–N3	2.10(2)
Sn2–N2	2.13(2)	Sn4–N4	2.10(2)
Sn2–O1	2.39(2)	Sn2–O1	2.40(2)
N1-Sn1-N2	85.0(7)	N3-Sn3-N4	83.6(7)
N1-Sn1-Se1	121.2(5)	N3-Sn3-Se2	119.7(5)
N2-Sn1-Se1	115.5(5)	N4-Sn3-Se2	121.1(4)
Se1-Sn1-Se1A	98.0(1)	Se2-Sn3-Se2A	98.4(1)
N1-Sn2-N2	79.4(7)	N3-Sn4-N4	80.5(6)
N1-Sn2-O1	94.6(6)	N3-Sn4-O2	92.0(6)

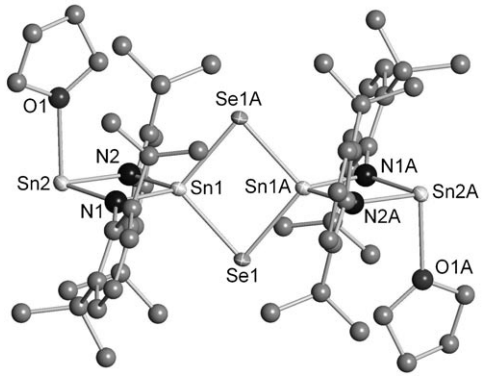

Figure 7. Molecular structure of complex **9**. Thermal ellipsoids are shown at 30% probability. Hydrogen atoms have been removed for clarity.

membered rings. There are two Sn_2N_2 rings, which are nearly planar (mean deviation from planarity: Sn1-N1-Sn2-N2 = 0.025 Å), that are bridged by a perfectly planar Sn_2Se_2 ring, which shares the tin centres. The Sn_2Se_2 ring is essentially orthogonal to the Sn_2N_2 rings (85.7°). The bridging Sn–Se distances range from 2.519(3)–2.557(3) Å, and are typical of Sn–Se single bond lengths.[19] As expected, the Sn^{IV}–N distances are shorter than the Sn^{II}–N distances (Table 2) due to the higher ionic character of the Sn^{IV}–N bonds. The geometries of the Sn^{IV} centres are highly distorted tetrahedral, with the bond angles ranging from 83.6(7) to 121.2(5)°. The Sn^{II} centres are three coordinate, each bound to two bridging imido nitrogen centres and one molecule of THF.

NMR characterisation: The room-temperature NMR spectra obtained for magnesium complex **4** were consistent with the local C_3 symmetry of the cluster. For example, two resonances are observed in the expected 3:1 ratio for the two different μ_3-N*t*Bu groups in the ^{1}H NMR spectrum, and a single resonance is observed in the ^{119}Sn NMR spectrum. The ^{1}H NMR spectra for monochalcogenides **5a** and **5b** also displayed two resonances in a 3:1 ratio for the μ_3-N*t*Bu groups, rather than the expected 1:2:1 pattern. Consistently, only two sets of resonances for the μ_3-N*t*Bu groups are observed in the ^{13}C NMR spectra. The ^{119}Sn NMR spectrum for monoselenide derivative **5a** displays two resonances at $\delta = 334$ and -83 ppm in a 2:1 ratio for the Sn^{II} and Sn^{IV} centres, respectively, which is in keeping with the solid-state structure. However, satellites due to ^{119}Sn,^{77}Se coupling are only observed in the ^{119}Sn NMR spectrum at -30°C (Table 3). A single resonance is observed at $\delta = -46$ ppm in

Table 3. Correlation of multinuclear NMR data and Sn=E bonds lengths.

Complex	δ ^{119}Sn	$^1J_{SnE}$	Sn=E [Å][a]
(Se)Sn_3Mg (**5a**)	334, −83	3145	2.393(1)
(Se)Sn_3Li (**6a**)	386, −44	2684	2.452(1)
$(Se)_3Sn_3$Li (**3a′**)	−133	3200	2.386(1)–2.397(1)
(Te)Sn_3Li (**6b**)	399, −294	7022	2.640(1)
$(Te)_2Sn_3$Li (**7b″**)	234, −376	7580	2.614(1)–2.615(1)
$(Te)_3Sn_3$Li (**3b**)	−439	8400	2.607(1)[d]
[{η^4-Me_8(taa)}Sn=Se][b]	−444	3450	2.394(1)
[{CH($SiMe_3$)C_9H_6N-8}$_2$Sn=Se][c]	−112	2951	2.398(1)
[{CPh($SiMe_3$)C_9H_6N-2}$_2$Sn=Se][c]	−179	2682	2.418(1)
[{CH($SiMe_3$)C_9H_6N-8}$_2$Sn=Te][c]	−350	7808	2.618(1)

[a] E = Se, Te. [b] See ref. [18c]. η^4-Me_8(taa) = octamethyldibenzotetraaza[14]annulene. [c] See ref. [5]. [d] This is the average Sn=Te bond length, taken from 18 Sn=Te lengths ranging from 2.600(1)–2.613(1) Å.

the ^{77}Se NMR spectrum. The room-temperature ^{119}Sn NMR spectrum for monotelluride **5b** contains no observable resonances, nor could any resonance be detected in the ^{125}Te NMR spectrum. However, when the temperature of the NMR solution is reduced to -50°C, broad resonances are observed at $\delta = 356$ and -354 ppm in the ^{119}Sn NMR spectrum, which are assigned to the Sn^{II} and Sn^{IV} centres, respectively. Concomitant with the appearance of these resonances, a single resonance at $\delta = -568$ ppm appears in the ^{125}Te NMR spectrum. The NMR data obtained for **5a** and **5b** suggest that there is rapid exchange of the chalcogen atom between all three tin centres, which has been previously observed to occur in related systems.[6,12] It has been observed that the rate of exchange in tin complexes increases along the series of chalcogens in the order of S < Se < Te.[12,20] The more facile exchange of tellurium relative to selenium is most apparent in the ^{119}Sn NMR data of **5a** and **5b**, for which only broad resonances could be observed at low temperature for monotelluride **5b**, whereas sharp resonances, including ^{77}Se satellites, are observed for **5a**.

In contrast to the magnesium-containing complexes, the NMR spectra of lithium-containing complexes **6** and **7** are well-resolved at room temperature. For monochalcogenide complexes **6a** and **6b**, the ^{1}H NMR spectra each display two resonances in a 3:1 ratio for the μ_3-N*t*Bu groups rather than the expected 1:2:1 pattern, similar to complexes **5a** and **5b**. The ^{13}C NMR spectrum of **6a** displays two sets of three resonances for the μ_3-N*t*Bu groups, while for **6b** there are two sets of only two resonances each. For both of the complexes, the room-temperature ^{119}Sn NMR spectra contain two resonances corresponding to the Sn^{II} and Sn^{IV} centres in the expected 2:1 pattern with sharp ^{77}Se and ^{125}Te satellites accom-

panying the Sn^{IV} resonance (Table 3). A single, sharp resonance with well-resolved $^{117}Sn/^{119}Sn$ satellites is observed in the ^{77}Se and ^{125}Te NMR spectra of complexes **6a** and **6b**, respectively (Table 3).

While it is not possible to establish unambiguously if the dimeric structure of **6a** is maintained in solution, the ^{13}C and, in particular, the ^{7}Li NMR data provide valuable information. The ^{7}Li NMR resonance for the noncage lithium atom appears at $\delta = 0.01$ ppm, which is considerably shifted from the analogous resonances for the other lithium complexes ($\delta = -0.53$ to -0.70 ppm). Thus, the presence of the expected two sets of three ^{13}C NMR resonances for the *t*Bu groups and the unique ^{7}Li NMR shift observed for the noncage lithium atom, suggest that the dimeric structure for **6a** is maintained, even in THF. For complex **6a**, if the dimeric structure is maintained in solution, it seems unlikely that chalcogen exchange could easily occur, which could account for the difference in the ^{13}C NMR spectra observed for complexes **6a** and **6b**. The well-resolved room-temperature NMR data obtained for complexes **6a** and **6b** suggest that if chalcogen exchange is occurring, it is slow on the NMR timescale.

The NMR data obtained for diselenide **7a** are in keeping with the solid-state structure obtained for **7b**″. The ^{1}H NMR spectrum shows the expected 1:2:1 pattern for the methyl protons of the three different N*t*Bu groups; this pattern is also present in the ^{13}C NMR spectrum. For complex **7b**, the ^{1}H and ^{13}C NMR spectra only show two resonances for the N*t*Bu groups, however, in each case one of the resonances observed is broad, and is likely a result of poorly resolved overlap of two separate resonances. The ^{119}Sn NMR spectra for each of the complexes (**7a** and **7b**) exhibit resonances for the Sn^{II} and Sn^{IV} centres in the expected 1:2 intensities, respectively. The resonance for the Sn^{IV} centre displays the appropriate ^{77}Se (**7a**) or ^{125}Te (**7b**) satellites.

The well-characterised series of complexes containing tin–chalcogen terminal bonds reported in this work allows for a comparison of the structural and NMR data. These data are compiled in Table 3 and are compared with pertinent data for related complexes previously reported in the literature. It is readily apparent that there is an inverse relationship between the observed ^{1}J(Sn,E) coupling constants and the Sn=E bond lengths. Along the series of stannatellurones **6b**, **7b**″ and **3b** there is a marked increase in the magnitude of the ^{1}J(Sn,Te) coupling constants concomitant with a steady decrease in the Sn=Te bond length. However, there does not appear to be a direct relationship between the absolute magnitude of a one-bond coupling constant and the observed terminal bond length. For example, the observed Sn=Se bond length of 2.394(1) Å for complex [Sn=Se{η^4-Me_8(taa)}] is identical to that observed in **5a** (2.393(1) Å), but the coupling constants are 3450 and 3145 Hz, respectively. Nonetheless, it is clear that within a closely related series of complexes, there is a direct correlation between the magnitude of the coupling constants and the Sn=E bond lengths.

The NMR data obtained for complex **9** are consistent with the solid-state structure. In the ^{1}H NMR spectrum, one doublet is observed for the methyl protons of the isopropyl groups, as well as a septet for the methine protons, indicating equivalence of the four 2,6-diisopropylphenyl groups. The ^{119}Sn NMR spectrum displays two resonances of equal intensity for the Sn^{II} and Sn^{IV} centres; there is a single resonance in the ^{77}Se NMR spectrum. Unfortunately, we were unable to observe the $^{1}J(^{119}Sn,^{77}Se)$ coupling because of the very low solubility of this complex.

Conclusion

This investigation demonstrates that the anionic lithium-containing cubane $[Sn_3Li(\mu_3\text{-}NtBu)_4]^-$ is substantially more reactive towards heavy chalcogens than the analogous, neutral magnesium-containing complex $[Sn_3Mg(\mu_3\text{-}NtBu)_4]$. This finding parallels our previous observations on the reactivity of the phosphorus(III) systems $Li_2[tBuNP(\mu\text{-}NtBu)_2PNtBu]$ and $Mg[tBuNP(\mu\text{-}NtBu)_2PNtBu]$ towards tellurium.[26] In that work, however, both complexes are neutral whereas in the current work the lithium-containing complex is anionic. The anionic character renders the Sn^{II} centres dramatically more nucleophilic so that trichalcogenides are easily obtained under mild conditions. The catalytic role of the anion $[Sn_3Li(\mu_3\text{-}NtBu)_4]^-$ in chalcogen-transfer reactions is also an intriguing observation that may have wider applications. The lithium-containing trichalcogenides $[E_3Sn_3Li(\mu_3\text{-}NtBu)_4]^-$ (E = Se, Te) merit further study as stoichiometric reagents for the incorporation of other metals, for example, Ge or Pb, to give neutral heterobimetallic cubanes that may serve as single-source precursors of ternary chalcogenides. Finally, the first example of the dissociation of a Sn_4N_4 imidotin cubane into two Sn_2N_2 rings is reported. The implications of this transformation, including the reactivity of the tin(II) centres in the product so obtained, will be pursued.

Experimental Section

All reactions and the manipulations of products were performed under an argon atmosphere by using standard Schlenk techniques or an inert-atmosphere glove box. Solvents were freshly distilled, dried and degassed prior to use. Rigorous precautions are necessary for handling complexes **2a** and **2b**, because they are very sensitive to air and moisture. NMR spectra were obtained with sample solutions in [D_8]THF at 25 °C using a Bruker AMX 300 spectrometer, unless otherwise noted. ^{77}Se, ^{119}Sn and ^{125}Te NMR spectra were referenced to the external standards $(SePh)_2$, $SnMe_4$ and $(TePh)_2$, respectively. The reagents $[Sn_3(\mu_3\text{-}NtBu)(\mu_2\text{-}NtBu)(\mu_2\text{-}NHtBu)_2]$ (**1**),[10] $[Sn_3Li(\mu_3\text{-}NtBu)_4][Li(thf)_4]$ (**2a**),[11] $[Sn_3Li(\mu_3\text{-}NtBu)_4][(thf)Li([12]crown\text{-}4)]$ (**2a**′)[11] and $[\{SnN(dipp)\}_4]$ (**8**)[15] were prepared as previously reported. The complex $[Sn_3Li(\mu_3\text{-}NtBu)_4][Li([12]\text{-}crown\text{-}4)_2]$ (**2a**″) was prepared by reaction of **2a** with 2 equiv of [12]crown-4.[11] The complex $[Sn_3Te_3Li(\mu_3\text{-}NtBu)_4][Li([12]crown\text{-}4)_2]$ (**3b**″) was prepared by reaction of **2a**″ with 3 equiv of tellurium.[11]

Compound 4: To a solution of **1** (5.80 g, 9.0 mmol) in THF (80 mL), dibutylmagnesium (1.0 M in heptane, 15.0 mL, 15.0 mmol) was added and the solution was heated to 60 °C for 16 h. The solvent was removed in vacuo and the yellow residue was washed with hexanes (2 × 50 mL). The remaining solid was dissolved in THF (40 mL), filtered and the solution was concentrated to approximately 20 mL. Storage of the solution at 5 °C

for 12 h resulted in the deposition of pale-yellow crystals of **4** (4.60 g, 69%). ^{1}H NMR: δ=1.35 (s, 9H; N*t*Bu), 1.40 (s, 27H; N*t*Bu), 1.78 (m, 4H; THF), 3.64 ppm (m, 4H; THF); ^{13}C NMR: δ=26.34 (THF), 27.13, 36.13 (C(CH_3)$_3$), 54.60, 54.69 (C(CH_3)$_3$), 68.22 ppm (THF); ^{119}Sn NMR: δ=508 ppm (s); elemental analysis calcd (%) for $C_{20}H_{44}N_4MgOSn_3$ (737.03): C 32.59, H 6.02, N 7.60; found: C 32.40, H 6.26, N 7.24.

Compound 5a: A mixture of **4** (0.300 g, 0.41 mmol) and grey selenium powder (0.032 g, 0.041 mmol) in THF (20 mL) was stirred at room temperature for 1 h. The resulting pale-yellow solution was filtered through a filter disk (0.45 μm pore size) and the solution was concentrated to approximately 5 mL. Storage of the solution at 5°C for 12 h resulted in the deposition of pale-yellow crystals of **5a** (0.180 g, 54%). ^{1}H NMR: δ= 1.39 (s, 9H; N*t*Bu), 1.45 (s, 27H; N*t*Bu), 1.77 (m, 4H; THF), 3.62 ppm (m, 4H; THF); ^{13}C NMR: δ=26.32 (THF), 30.99, 36.73 (C(CH_3)$_3$), 55.52, 56.73 (C(CH_3)$_3$), 68.22 ppm (THF); ^{77}Se NMR: δ=−46 ppm (s); ^{119}Sn NMR (−30°C): δ=−83 (s, ^2J(Sn,Sn)=218 Hz, ^1J(Sn,Se)=3145 Hz 1Sn), 334 ppm (s, 2Sn); elemental analysis calcd (%) for $C_{20}H_{44}N_4MgOSeSn_3$ (815.99): C 29.44, H 5.44, N 6.87; found: C 27.39, H 5.08, N 6.63.

Compound 5b: A mixture of **4** (0.310 g, 0.42 mmol) and tellurium powder (0.060 g, 0.47 mmol) in THF (30 mL) was stirred at 40°C for 3 h. The resulting orange solution was filtered though a filter disk (0.45 μm pore size) and the solution was concentrated to approximately 5 mL. Addition of diethyl ether (40 mL) resulted in the precipitation of **5b** as a fine orange powder (0.278 g, 76%). ^{1}H NMR: δ=1.41 (s, 9H; N*t*Bu), 1.43 (s, 27H; N*t*Bu), 1.78 (m, 4H; THF), 3.62 ppm (m, 4H; THF); ^{13}C NMR: δ=26.32 (THF), 30.15, 36.05 (C(CH_3)$_3$), 55.89, 56.82 (C-(CH_3)$_3$), 68.22 ppm (THF); ^{119}Sn NMR (−50°C): δ=−354 (br), 356 ppm (br); ^{125}Te NMR (−50°C): δ=−568 ppm (br); elemental analysis calcd (%) for $C_{20}H_{44}N_4MgOSn_3Te$ (864.62): C 27.78, H 5.12, N 6.48; found: C 27.89, H 4.77, N 6.86. X-ray quality crystals of **5b** were obtained by the slow evaporation of solvent from a solution of the complex in benzene.

Compound 6a

Method A: A mixture of **2a** (0.200 g, 0.20 mmol) and grey selenium powder (0.016 g, 0.20 mol) in THF (20 mL) was stirred at room temperature for 5 min. The resulting pale-yellow solution was filtered though a filter disk (0.45 μm pore size) and the solvent was removed in vacuo. The solid was dissolved in diethyl ether (10 mL) then concentrated to approximately 2 mL resulting in the precipitation of **6a** as a pale-yellow powder (0.129 g, 69%).

Method B: A mixture of **3a** (0.150 g, 0.12 mmol) and **2a** (0.243 g, 0.24 mmol) in THF (20 mL) was stirred at room temperature for 15 min; workup followed the procedure described for method A (0.290 g, 85%). ^{1}H NMR: δ=1.32 (s, 9H; N*t*Bu), 1.35 (s, 27H; N*t*Bu), 1.77 (m, 12H; THF), 3.63 ppm (m, 12H; THF); ^{7}Li NMR: δ=0.01 (s; μ$_2$-Li(thf)$_2^+$), 1.84 ppm (s; [(thf)LiSn$_3$(N*t*Bu)$_4$]$^-$); ^{13}C NMR: δ=26.37 (THF), 30.83, 37.11, 37.29 (C(CH_3)$_3$), 55.42, 56.11, 56.24 (C(CH_3)$_3$), 68.37 ppm (THF); ^{77}Se NMR: δ=−158 ppm (s, ^1J(^{119}Sn,Se)=2689 Hz, ^1J(^{117}Sn,Se)= 2571 Hz); ^{119}Sn NMR: δ=−44 (s, ^1J(Sn,Se)=2684 Hz, 1Sn), 386 ppm (s, 2Sn); elemental analysis calcd (%) for $C_{56}H_{120}N_8Li_4O_6Se_2Sn_6$ (1899.55): C 35.41, H 6.37, N 5.90; found: C 34.42, H 6.19, N 6.38. X-ray quality crystals of **6a** were grown from a concentrated solution of the complex in diethyl ether stored at −10°C for 24 h.

Compound 6b: This was prepared similarly to **6a** (method B) from **3b** (0.150 g, 0.11 mmol) and **2a** (0.218 g, 0.22 mmol) to give **6b** as an orange powder (0.247 g, 67%). ^{1}H NMR: δ=1.36 (s, 27H; N*t*Bu), 1.38 (s, 9H; N*t*Bu), 1.79 (m, 20H; THF), 3.63 ppm (m, 20H; THF); ^{7}Li NMR: δ= −0.57 (s; Li(thf)$_4^+$), 1.92 ppm (s; [(thf)LiSn$_3$(N*t*Bu)$_4$]$^-$); ^{13}C NMR: δ= 26.45 (THF), 29.84, 37.14 (C(CH_3)$_3$), 55.81, 56.48 (C(CH_3)$_3$), 68.38 ppm (THF); ^{119}Sn NMR: δ=−299 (s, ^1J(Sn,Te)=7022 Hz, 1Sn), 399 ppm (s, 2Sn); ^{125}Te NMR: δ=−659 ppm (s, ^1J(^{119}Sn,Te)=7012 Hz, ^1J(^{117}Sn, Te)= 6696 Hz); elemental analysis calcd (%) for **6b** (with loss of one THF) $C_{32}H_{68}N_4Li_2O_4Sn_3Te$ (1070.52): C 35.90, H 6.40, N 5.23; found: C 36.17, H 6.46, N 5.52. X-ray quality crystals of **6b** were obtained by slow diffusion of *n*-hexane into a solution of the complex in THF at 5°C.

Compound 7a: This was prepared similarly to **6a** (method B) from **3a** (0.079 g, 0.063 mmol) and **2a** (0.032 g, 0.032 mmol) to give **7a** as a pale-yellow powder (0.092 g, 83%). ^{1}H NMR: δ=1.37 (s, 18H; N*t*Bu), 1.43 (s, 9H; N*t*Bu), 1.49 (s, 9H; N*t*Bu), 1.77 (m, 20H; THF), 3.63 ppm (m, 20H; THF); ^{7}Li NMR: δ=−0.53 (s; Li(thf)$_4^+$), 1.62 ppm (s; [(thf)LiSn$_3$-(N*t*Bu)$_4$]$^-$); ^{13}C NMR: δ=26.33 (THF), 32.96, 36.73, 37.12 (C(CH_3)$_3$), 56.12, 57.30, 57.78 (C(CH_3)$_3$), 68.36 ppm (THF); ^{77}Se NMR: δ= −142 ppm (s, ^1J(^{119}Sn,Se)=2984 Hz, ^1J(^{117}Sn,Se)=2852 Hz); ^{119}Sn NMR: δ=−86 (s, ^1J(Sn,Se)=2988 Hz, 2Sn), 197 ppm (s, 1Sn); elemental analysis calcd (%) for **7a** (with loss of one THF) $C_{32}H_{68}N_4Li_2O_4Se_2Sn_3$ (1100.84): C 34.91, H 6.23, N 5.09; found: C 34.63, H 6.02, N 4.88.

Compound 7b: A mixture of **3b** (0.400 g, 0.29 mmol) and **2a** (0.145 g, 0.14 mmol) in THF (20 mL) was stirred at room temperature for 15 min. The solution was filtered though a filter disk (0.45 μm pore size), concentrated to approximately 5 mL and diethyl ether (50 mL) was added. The solution was stirred vigorously for 1 h, during which time **7b** precipitated as a bright-orange powder (0.460 g, 84%). ^{1}H NMR: δ=1.41 (br s, 27H; N*t*Bu), 1.46 (s, 9H; N*t*Bu), 1.78 (m, 20H; THF), 3.63 ppm (m, 20H; THF); ^{7}Li NMR: δ=−0.64 (s; Li(thf)$_4^+$), 1.75 ppm (s; [(thf)LiSn$_3$-(N*t*Bu)$_4$]$^-$); ^{13}C NMR: δ=26.28 (THF), 31.57, 36.97 (C(CH_3)$_3$), 56.93, 58.11 (C(CH_3)$_3$), 68.22 ppm (THF); ^{119}Sn NMR: δ=−382 (s, ^1J(Sn,Te)= 7604 Hz, 2Sn], 234 ppm (s, 1Sn); ^{125}Te NMR: δ=−313 ppm (s, ^1J(^{119}Sn,Te)=7620 Hz, ^1J(^{117}Sn,Te)=7300 Hz); elemental analysis calcd (%) for $C_{36}H_{76}N_4Li_2O_5Sn_3Te_2$ (1270.22): C 34.04, H 6.03, N 4.41; found: C 33.90, H 5.67, N 4.44.

Compound 7b″: A mixture of **3b″** (0.200 g, 0.14 mmol) and **2a″** (0.074 g, 0.07 mmol) in THF (20 mL) was stirred at room temperature for 15 min. The solution was filtered though a filter disk (0.45 μm pore size), concentrated to approximately 5 mL and diethyl ether (50 mL) was added, precipitating **7b″** as an orange powder (0.221 g, 81%). ^{1}H NMR: δ=1.42 (br s, 27H; N*t*Bu), 1.46 (s, 9H; N*t*Bu), 1.78 (m, 4H; THF), 3.63 (m, 4H; THF), 3.75 ppm (s, 32H; [12]crown-4); ^{119}Sn NMR: δ=−376 (s, ^1J(Sn,Te)=7580 Hz, 2Sn), 234 ppm (s, 1Sn); ^{125}Te NMR: δ=−615 ppm (s). X-ray quality crystals were grown from a concentrated solution of the complex in THF at 5°C.

Compound 9: A mixture of **8** (1.000 g, 0.85 mmol), **2a** (0.050 g, 0.05 mmol) and Se (0.140 g, 1.77 mmol) in THF (15 mL) was stirred at room temperature for 24 h, during which time **9** precipitated as a yellow crystalline solid. The solution was concentrated to approximately 5 mL and then the solvent was decanted off, and the crystals of **9** were dried (0.728 g, 58%). ^{1}H NMR (C_6D_6): δ=1.23 (d, ^3J(H,H)=7 Hz, 48H; CH-(CH_3)$_2$), 1.34 (m, 8H; THF), 3.50 (m, 8H; THF), 3.91 ppm (m, 8H; C*H*-(CH_3)$_2$) 7.05 ppm (m, 12H; C_6H_3); ^{119}Sn NMR: δ=−147 (s; Sn^{IV}-Se), 329 ppm (s; Sn^{II}); ^{77}Se NMR: δ=344 ppm (s); elemental analysis calcd (%) for $C_{56}H_{84}N_4O_2Sn_4Se_2$ (1478.05): C 45.51, H 5.73, N 3.79; found: C 44.93, H 5.48, N 3.76. X-ray quality crystals of **9** were grown from slow diffusion of *n*-hexane into a solution of the complex in THF at 5°C.

X-ray structural determinations: A suitable crystal of the complex was selected, coated in Paratone oil and mounted on a glass fibre. Data were collected at 173 K on a Nonius Kappa CCD diffractometer using $Mo_{K\alpha}$ radiation (λ=0.71073 Å) with ω and φ scans. The unit-cell parameters were calculated and refined from the full data set. Crystal cell refinement and data reduction were carried out by using the Nonius DENZO package. After data reduction, the data were corrected for absorption based on equivalent reflections using SCALEPACK (Nonius, 1998). The structures were solved by direct methods using SHELXS-97 and refinement was carried out on F^2 against all independent reflections by the full-matrix least-squares method using the SHELXL-97 program.[21] The hydrogen atoms were calculated geometrically and were riding on their respective atoms. Except as mentioned, all non-hydrogen atoms were refined with anisotropic thermal parameters. Crystal data are summarised in Tables 4 and 5. CCDC-278735 to CCDC-278741 contain the supplementary crystallographic data for this paper. These data can be obtained free of charge from the Cambridge Crystallographic Data Centre via www.ccdc.cam.ac.uk/data_request/cif.

Compound 4: The molecule was well ordered, with the exception of the coordinated THF molecule, which was disordered over two positions and was modelled as a 50:50 anisotropic mixture. The solvent of crystallisation was disordered across a crystallographic mirror plane and was modelled as an isotropic 50:50 mixture. In both cases, mild geometric restraints were applied. Owing to symmetry, only one half of the molecule

Table 4. Crystal data and structure refinements for complexes **4**, **5a**, **5b** and **6a**.

	4	**5a**	**5b**	**6a**
empirical formula	$C_{20}H_{44}MgN_4OSn_3{\cdot}C_4H_8O$	$C_{40}H_{88}Mg_2N_4O_2Se_2Sn_6{\cdot}C_4H_8O$	$C_{20}H_{44}MgN_4OSn_3Te{\cdot}0.5(C_6H_6)$	$C_{56}H_{120}Li_4N_8O_6Se_2Sn_6$
formula weight	809.08	1703.97	903.63	1899.42
crystal system	orthorhombic	monoclinic	monoclinic	monoclinic
space group	*Pnma*	$P2_1/c$	$P2_1/c$	$P2_1/n$
a [Å]	18.963(4)	31.190(6)	15.686(3)	10.724(2)
b [Å]	11.448(2)	10.875(2)	11.005(2)	20.019(4)
c [Å]	15.591(3)	19.066(4)	18.932(4)	18.976(4)
β [°]		91.64(3)	91.59(3)	90.94(3)
V [Å^3]	3385(1)	6464(2)	3267(1)	4073(1)
Z	4	4	4	2
ρ_{calcd} [g cm^{-3}]	1.588	1.751	1.837	1.549
μ ($Mo_{K\alpha}$) [mm^{-1}]	2.239	3.467	3.191	2.748
reflections collected	23359	41178	36316	60426
independent reflections	4035	13926	7431	8323
parameters	185	591	298	345
goodness-of-fit on F^2	1.037	1.035	1.026	1.021
final R indices [$I>2\sigma(I)$] R_1, wR_2	0.0279, 0.0709	0.0476, 0.0802	0.0335, 0.0711	0.0350, 0.0807
R indices (all data) R_1, wR_2	0.0372, 0.0753	0.0949, 0.0917	0.0539, 0.0777	0.0540, 0.0883
largest diff. peak/hole [e Å^{-3}]	0.788/−0.532	0.738/−0.819	1.290/−1.025	1.273/−1.1

Table 5. Crystal data and structure refinements for complexes **6b**, **7b″** and **9**.

	6b	**7b″**	**9**
empirical formula	$C_{36}H_{76}Li_2N_4O_5Sn_3Te$	$C_{36}H_{76}Li_2N_4O_9Sn_3Te_2{\cdot}C_4H_8O$	$C_{56}H_{84}N_4O_2Sn_4Se_2$
formula weight	1142.56	1406.26	1477.95
crystal system	monoclinic	orthorhombic	triclinic
space group	$C2/c$	*Pbca*	$P\bar{1}$
a [Å]	17.701(4)	15.247(3)	13.275(3)
b [Å]	14.370(3)	15.339(3)	13.355(3)
c [Å]	39.214(8)	47.56(1)	17.794(4)
α [°]			89.81(3)
β [°]	99.73(3)		76.70(3)
γ [°]			89.46(3)
V [Å^3]	9831(4)	11122(4)	3070(1)
Z	8	8	2
ρ_{calcd} [g cm^{-3}]	1.544	1.680	1.599
μ ($Mo_{K\alpha}$) [mm^{-1}]	2.132	2.415	2.834
reflections collected	31102	55441	53248
independent reflections	8253	10092	10784
parameters	430	371	304
goodness-of-fit on F^2	1.060	1.083	1.053
final R indices [$I>2\sigma(I)$] R_1, wR_2	0.0445, 0.0808	0.0740, 0.1323	0.0687, 0.1306
R indices (all data) R_1, wR_2	0.0763, 0.0905	0.1415, 0.1524	0.1302, 0.1584
largest diff. peak/hole [e Å^{-3}]	0.807/−0.705	1.578/−0.866	0.893/−0.941

was located in the difference Fourier map, as the molecule is situated on a crystallographic mirror plane.

Compound ***5a***: The complex crystallises with two independent but chemically equivalent molecules in the asymmetric unit.[22] The molecules were well ordered, with the exception of the coordinated THF molecules. One coordinated THF was modelled as a 40:30:30 isotropic mixture of all carbon atoms, while the second coordinated THF was modelled with a 60:40 disorder of two carbon atoms; in each case mild geometric restraints were applied. The lattice-bound THF molecule was modelled as a 75:25 isotropic mixture with geometric restraints.

Compound ***5b***: No special considerations.

Compound ***6a***: The molecule was well ordered, with the exception of two coordinated THF molecules. One disordered THF was modelled as a 75:25 isotropic mixture with mild geometric restraints. The second THF was highly disordered and the best model that could be refined was a 60:20:20 isotropic mixture with geometric restraints. The lithium atoms were refined with isotropic thermal parameters. Owing to symmetry, only one half of the molecule was located in the difference Fourier map, as the molecule is situated on a crystallographic centre of inversion.

Compound ***6b***: The molecule was well ordered, with the exception of two coordinated THF molecules. One disordered THF was modelled as a 35:35:30 isotropic mixture, while the second was modelled as a 65:35 isotropic mixture; in each case mild geometric restraints were applied. The lithium atoms were refined with isotropic thermal parameters.

Compound ***7b″***: The anionic cluster was well ordered, with the exception of the coordinated THF molecule, which had a positional disorder of one of the carbon atoms, and was modelled as a 75:25 isotropic mixture. The crown ether molecules of the cation were disordered, and nearly all the carbon and oxygen atoms were modelled with a 50:50 positional disorder and refined isotropically. The lattice-bound molecule of THF was very poorly ordered and was modelled as an isotropic 50:50 mixture. Only the heavy atoms (Sn, Te) of the anionic cluster were refined with anisotropic thermal displacement parameters. The crystals of the complex formed as pseudotetragonal merohedral twins. The twin law (010, 100, 00−1) was applied in the final refinement stages using the TWIN instruction, which resulted in significant improvement of the R values, K value, estimated standard deviations (esds) and background noise.

Compound ***9***: The complex crystallises with two independent, but chemically equivalent molecules in the unit cell, for which two independent halves of the molecules are present in the asymmetric unit (the other half in each case being generated by the crystallographic inversion centre). The refinement was complicated by twinning of the data and only the heavy atoms could be refined with anisotropic thermal parameters. There were many indications of twinning, including the fact that the refinement stalled at 12.09%. Application of the twin determination program ROTAX determined that twinning occurred around the [001] direct lat-

tice axis.[23] The program WinGX was used to prepare an HKLF5 file for further refinement.[24] The *R* values, *K* value, esds and background noise were all improved, indicating the correct twin assignment.

Acknowledgements

The authors gratefully acknowledge financial support from the Natural Sciences and Engineering Research Council (Canada) and the Alberta Ingenuity Fund.

[1] For reviews, see: a) N. Tokitoh, R. Okazaki, in *The Chemistry of Organic Germanium, Tin and Lead Compounds, Vol. 2*, Part 1, (Ed.: Z. Rapoport), Wiley, Chichester, UK, **2002**, p. 843; b) N. Tokitoh, R. Okazaki, *Adv. Organomet. Chem.* **2001**, *47*, 121–166; c) R. Okazaki, N. Tokitoh, *Acc. Chem. Res.* **2000**, *33*, 625–630; d) P. P. Power, *Chem. Rev.* **1999**, *99*, 3463–3503.

[2] a) For tin–selenium double bonds (stannaneselones), see: M. Saito, N. Tokitoh, R. Okazaki, *J. Am. Chem. Soc.* **2004**, *126*, 15572–15582, and references therein; b) Terminal tin–tellurium bonds involving three-coordinate tin (stannanetellones) have not been obtained by using this approach.

[3] The term "heavy ketone" has been used to describe this class of compounds (see ref. [1]).

[4] T. Chivers, G. Schatte, *Chem. Commun.* **2001**, 2264–2265.

[5] W.-P. Leung, W.-H. Kwok, Z.-Y. Zhou, T. C. W. Mak, *Organometallics* **2000**, *19*, 296–303.

[6] T. Chivers, T. J. Clark, M. Krahn, M. Parvez, G. Schatte, *Eur. J. Inorg. Chem.* **2003**, 1857–1860.

[7] For examples, see: a) C. An, K. Tang, B. Hai, G. Shen, C. Wang, Y. Qian, *Inorg. Chem. Commun.* **2003**, *6*, 181–184; b) S. Schlecht, M. Budde, L. Kienle, *Inorg. Chem.* **2002**, *41*, 6001–6005; c) Y. Li, Z. Wang, Y. Ding, *Inorg. Chem.* **1999**, *38*, 4737–4740.

[8] a) P. Boudjouk, M. P. Remington, Jr., D. G. Grier, W. Triebold, B. R. Jarabek, *Organometallics* **1999**, *18*, 4534–4537; b) A. L. Seligson, J. Arnold, *J. Am. Chem. Soc.* **1993**, *115*, 8214–8220.

[9] G. G. Briand, T. Chivers, M. Parvez, *Angew. Chem.* **2002**, *114*, 3618–3620; *Angew. Chem. Int. Ed.* **2002**, *41*, 3468–3470.

[10] M. Veith, M.-L. Sommer, D. Jäger, *Chem. Ber.* **1979**, *112*, 2581–2587.

[11] T. Chivers, D. J. Eisler, *Angew. Chem.* **2004**, *116*, 6854–6857; *Angew. Chem. Int. Ed.* **2004**, *43*, 6686–6689.

[12] T. Chivers, D. J. Eisler, J. S. Ritch, *Z. Anorg. Allg. Chem.* **2004**, *630*, 1941–1946.

[13] G. G. Briand, T. Chivers, M. Parvez, G. Schatte, *Inorg. Chem.* **2003**, *42*, 525–531.

[14] V. Jancik, M. M. Moya Cabrera, H. W. Roesky, R. Herbst-Irmer, D. Neculai, A. M. Neculai, M. Noltemeyer, H.-G. Schmidt, *Eur. J. Inorg. Chem.* **2004**, 3508–3512.

[15] H. Chen, R. A. Bartlett, H. V. R. Dias, M. M. Olmstead, P. P. Power, *Inorg. Chem.* **1991**, *30*, 3390–3394.

[16] M. Veith, W. Frank, *Angew. Chem.* **1984**, *96*, 163–164; *Angew. Chem. Int. Ed. Engl.* **1984**, *23*, 158–159.

[17] Y. Zhou, D. Richeson, *J. Am. Chem. Soc.* **1996**, *118*, 10850–10852.

[18] a) M. Saito, N. Tokitoh, R. Okazaki, *J. Am. Chem. Soc.* **1997**, *119*, 11124–11125; b) W.-P. Leung, W.-H. Kwok, L. T. C. Law, Z.-Y. Zhou, G. Parkin, *Chem. Commun.* **1996**, 505–506; c) M. C. Kuchta, G. Parkin, *J. Am. Chem. Soc.* **1994**, *116*, 8372–8373.

[19] M. Saito, N. Tokitoh, R. Okazaki, *J. Am. Chem. Soc.* **2004**, *126*, 15572–15582.

[20] L. M. Berreau, L. K. Woo, *J. Am. Chem. Soc.* **1995**, *117*, 1314–1317.

[21] G. M. Sheldrick, SHELXL-97, Program for Refinement of Crystal Structures, University of Göttingen, Göttingen, Germany, **1997**.

[22] A test for higher symmetry using ADDSYM[23] detected a potential lattice halving. The data were reprocessed with the *a* axis halved, resulting in only a single molecule of the complex in the asymmetric unit. However, refinement of the structure using the smaller unit cell results in a highly disordered structure solution. Thus, the larger unit cell was used for complete refinement of the structure.

[23] R. I. Cooper, R. O. Gould, S. Parsons, D. J. Watkin, *J. Appl. Crystallogr.* **2002**, *35*, 168–174.

[24] L. J. Farrugia, *J. Appl. Crystallogr.* **1999**, *32*, 837–838.

[25] A. L. Spek, *PLATON, A Multipurpose Crystallographic Tool*, Utrecht University, Utrecht, The Netherlands, **2000**.

[26] G. G. Briand, T. Chivers, M. Parvez, G. Schatte, *Inorg. Chem.* **2003**, *42*, 525–531.

Received: July 20, 2005
Published online: October 25, 2005

